



¹. S. Mohamed EID

DYNAMIC ANALYSIS AND EXPERIMENTAL EVALUATION OF THE METAL PUSH BELT CVT

¹. AUTOMOTIVE AND TRACTORS ENGINEERING, FACULTY OF ENGINEERING, HELWAN UNIVERSITY, CAIRO, EGYPT

ABSTRACT: Most vehicle transmission systems control the ratio between engine speed and wheel speed using a fixed number of metal gears; the Continuously Variable Transmission (CVT) in currently available vehicles utilize a pair of variable-diameter pulleys connected by a belt or chain that can produce an infinite number of engine/wheel speed ratios for improve fuel consumption, drivability effectively, achieve both protection of earth environment and improvement vehicle performance sagging. The present research focuses on developing influence of loading conditions on the slip behavior and torque transmitting ability of the CVT. The model also investigates the range of clamping forces needed to initiate the transmission and to successfully meet the pressure requirements. The experimental setup and the instrumentation are present in detail; the measurement results are presented allowing for a more detailed description of the functional properties of the V-belt type variator, especially those related to reapply value of oil pressure by separate hydraulic unit and reduction ratio.

KEYWORDS: Metal-pushing belt CVT, Friction analysis of CVT, Torque transmission of CVT, Slip analysis in CVT, and experimental of CVT

INTRODUCTION

The Continuously Variable Transmission (CVT) is increasingly used in automotive applications. It has an advantage over conventional automatic transmissions, with respect to the large transmission ratio coverage and absence of comfort issues related to shifting events. This enables the engine to operate at more economic operating points. For this reason, CVT equipped cars are more economical than cars equipped with planetary gear automatic transmissions. The key advantages of a CVT that interest vehicle manufacturers and customers can be summarized as:

- Higher engine efficiency.
- Higher fuel economy.
- Smooth acceleration without shift shocks.
- Infinite gear ratios with a small number of parts.
- Easy to manufacture and low cost.
- Light and Compact.

The basic configuration of a metal V-belt CVT consists of two variable diameter pulleys connected by a power-transmitting device i.e. a metal V-belt. The pulley centers are a fixed distance apart. The pulley on the engine side is called the primary or the driver pulley. The other on the final drive (or the wheel side) is the secondary or the driven pulley. Since one of the sheaves on each pulley is movable, the application of an axial force on the movable pulley sheave allows the belt to move radially in the pulley groove. In addition to the radial motion, the belt also moves tangentially around the pulley under the influence of an applied torque. The metal V-belt is made of two series of thin steel bands holding together thin trapezoidal elements. The elements are connected to each other by a system of pegs and holes, a peg in the forward face of an element connected to a hole in the rear face of the element in front. Usually, an initial gap exists between the elements of the belt as they are not tightly pressed together.

Torque is transferred from the driver to the driven pulley by the pushing action of the elements. As the belt moves, an element is carried forward on the driver pulley due to the friction forces generated from the pulley. This forward motion of the element generates compressive forces as it pushes on the element ahead of it. On the driven side, the belt transfers torque to the driven pulley through friction. Due to the presence of friction between the band pack and the elements, the tensile forces in the bands also vary as the belt moves on the driver and driven pulleys. Thus, the operation of such a CVT is based on both the pulling and pushing mechanisms of the composite-structured belt.

BACKGROUND OF CVT

The metal V-belt, manufactured by Van Doorne's Transmission, consists of 400 steel elements and two sets of nine stacked steel bands [1]. The system consists of a primary pulley indirectly linked to the engine through a torque converter and a secondary pulley leading to the final drive gears and wheels. Two pressures, primary and secondary, are associated with the primary and secondary pulleys, respectively. The secondary pressure is the hydraulic supply, or line pressure. The primary pressure is in part dictated by a solenoid relief valve commanded by an electronic engine controller, and is directly related to the difference in primary and secondary pressures. Therefore, our intermediate control objective will be to specify the ratio of primary to secondary pulley speed by means of primary pressure solenoid valve counts. The primary control objective will be to achieve a desired engine speed, which we consider a known function of throttle angle and vehicle speed. We will use this desired engine speed to specify the desired ratio, and then use the desired ratio to specify control input. Thus backstepping control will be used to achieve our goal. Fig. 1 illustrates the basic arrangement of a metal V-belt CVT. The band pack runs over the belt elements, whereas the belt element contacts not only the band pack, but also the pulley sheave.

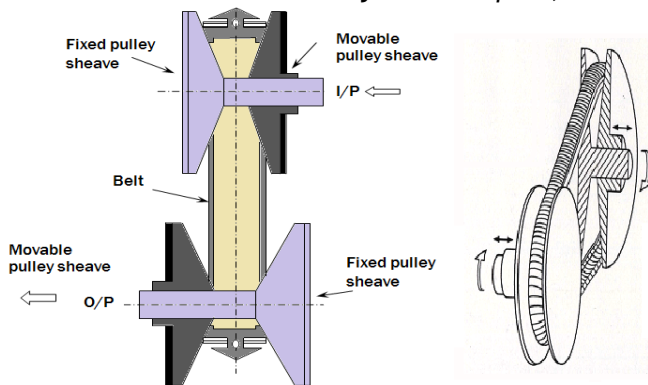


Fig. 1: Pulley arrangement

Continuously variable transmissions (CVTs) are typically composed of two hydraulically actuated variable radii pulleys and a metal pushing belt, the CVTs offer a continuum of infinitely variable gear ratios by changing the location of pulley sheaves. As a result, CVTs have the potential to increase the overall vehicle efficiency and reduce the jerk usually associated with manual and automatic transmissions. One shortcoming, however, is their difficulty in transmitting high torque at low operating speeds, which so far has limited their use to small vehicles.

CVT is an emerging automotive transmission technology that offers a continuum of gear ratios between high and low extremes. Today, Continuously Variable Transmissions have lured a great deal of automotive manufacturers and customers. Several car companies like Honda, Toyota, Ford, Nissan, etc., have been doing intensive research to exploit the advantages of a CVT. The chief advantage of a CVT is its ability to offer an infinite range of gear ratios with fewer moving parts, and consequently this influences engine efficiency, fuel economy, and cost.

A sundry of research is available on different aspects of a CVT, e.g. performance, slip behavior, efficiency, configuration design, loss mechanisms, vibrations, etc. Literature pertaining to the slip behavior of a belt CVT will be discussed subsequently. [2] Presented a unified slip theory based on the contributions of creep, compliance, shear deflection, and flexural rigidity of a rubber V-belt. Finite Element Analysis was used to calculate shear deflections in the belt and also to determine the stick-slip conditions on the belt. Incorporated the elastohydrodynamic lubrication theory to model friction between the metal belt and the pulley and also studied, both theoretically and experimentally, the influence of elemental gaps on the slip behavior of belt. The equilibrium conditions were assumed to develop a speed ratio-torque load-axial force relationship. The friction between the band and the elemental block was neglected. It was observed that the gross slip points depend on the torque transmission capacity of the driven side. Performance-based analyses of a metal V-belt drive and obtained a set of equations to describe the belt behavior based on quasi-static equilibrium. Coulomb friction model was used to model friction for all surfaces i.e. among individual bands, band element, and element-pulley. He also studied the deformation and creep of bands and blocks under the influence of torques and forces.

Historically slip in a CVT was regarded as destructive. The reason for this was that slip was not controllable and since it is unstable always resulted in damage to the variator. Recent publications suggest that limited amounts of slip in a push-belt type variator can be allowed [3]. This opens the door to other strategies for lowering the power consumption of CVT's. Not only can slip be used for optimizing variator efficiency actuation efficiency can also be greatly improved. If the safety margin is eliminated, the clamping force can be reduced by more than 25%. This can be directly translated into a 25% decrease in actuation power. Shifting behaviour is also influenced by slip [4]. This effect can be used to greatly reduce the power needed for fast shifting during emergency stopping, tip-shifting and kick down actions. Using this strategy the force needed for shifting is reduced, and with it the power needed from the actuation system is reduced. This has not only effects on the power consumed by the actuation system of the CVT, which is by itself a significant factor in the variator efficiency, but also has some implications on the design of the CVT. If actuation forces are smaller,

the actuation system can be smaller and cheaper, and the CVT itself will be lighter. Furthermore, other actuation systems than hydraulics can be considered, for example electromechanical actuation, to further enhance the controllability and efficiency of the actuation system. In this paper measurements are shown for shifting behaviour of the CVT and a relation will be given with slip in the system. The results are used to model the transient behavior of the CVT. [5] [6] analysed the shifting dynamics of a metal V-belt CVT under creep and sliding phases. They proposed a viscoplastic friction model to describe CVT dynamics in creep mode. They also studied the influence of clearance between the elements on the slip behavior of the belt.

The bands-segment interaction and the inertial effects of the belt were not modeled in detail. Non-dimensional equations were defined to encompass different loading scenarios. [7] Investigated elastic creep velocity of V-belt analytically and experimentally. The belt creep velocity depends not only on the structural characteristics of the belt, but also on the operational characteristics of the CVT. It was observed that the belt creep velocity was a function of transmitted power. The belt dynamics was modeled using quasi-static equilibrium concepts. [8] Investigated the torque transmitting capacity of a metal pushing V-belt CVT under no load condition on the driven pulley. Their research focused on the microslip behavior of the V-belt due to the redistribution of elemental gaps in the belt. [9] Developed a detailed dynamic model to understand the transient behavior and torque transmitting capacity of a metal V-belt CVT. The inertial coupling due to the radial and tangential motions of the belt was modeled in detail. Flexural effects were neglected and the contact between the belt and the pulley was modeled using continuous Coulomb friction theory. Their work illustrated the importance of belt inertial effects on the torque transmitting capacity of the metal V-belt CVT. They also emphasized on the significance of providing a feasible set of initial operating conditions to the CVT model in order to initiate torque transmission.

BELT GEOMETRY

The V-belt type variator appears in a few different forms. The difference is mostly the shape and materials used in the belt or chain and the shape of the pulleys. The pulley set on the input shaft, i.e. the engine side of the transmission, is referred to as the primary pulley; the pulley set on the output shaft is called the secondary pulley. Each pulley consists of a fixed and a moveable pulley sheave. [10], [11]. The primary and secondary moveable sheaves are on opposite sides of the belt, as also shown in Fig. 2 because mostly only one part of the pulley moves, the axial position of the belt is not constant.

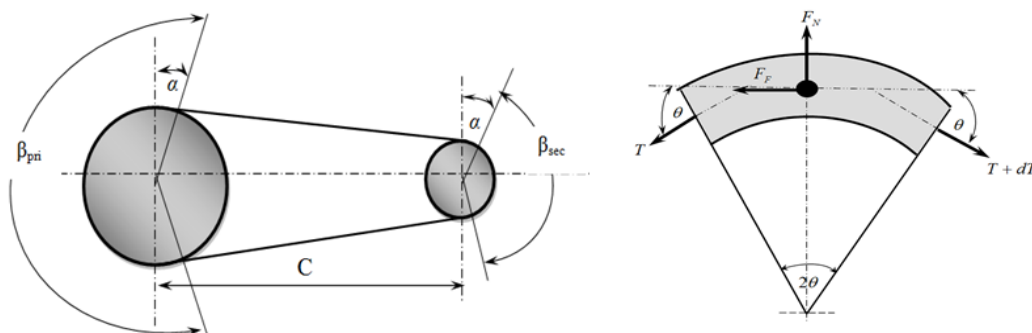


Fig. 2. Geometry of the Belt

$$L = \sqrt{4C^2 - (d_{sec} - d_{pri})^2} + \frac{1}{2}(d_{pri} \beta_{pri} + d_{sec} \beta_{sec}) \tag{1}$$

$$L = 2 * \sqrt{C^2 - (R_{sec} - R_{pri})^2} + R_{pri} \beta_{pri} + R_{sec} \beta_{sec} \tag{2}$$

Divide by C:

$$\frac{L}{C} = \sqrt{4 - \left(\frac{d_{sec} - d_{pri}}{C}\right)^2} + \frac{1}{2C}(d_{pri} \beta_{pri} + d_{sec} \beta_{sec}) \tag{3}$$

Since the length of the belt, L, is known, as is the distance between pulley centres C, the equation above can be implemented in an iterative program to find corresponding values of primary and second pulley diameters Rpri and Rsec and β_{pri} and β_{sec} for any value of belt ratio (i). In this work the belt ratio is defined in geometric terms, as output radius over input radius, as

$$i = \frac{R_{sec}}{R_{pri}} = \text{Transmission ratio} \tag{4}$$

$$\beta_{sec} = \pi + 2\alpha \text{ and } \beta_{pri} = \pi - 2\alpha$$

$$\sin \alpha = \frac{d_{sec} - d_{pri}}{2C} = \frac{R_{sec} - R_{pri}}{C} \tag{5}$$

$$\beta_{pri} = \pi - 2\sin^{-1}\left(\frac{d_{sec} - d_{pri}}{2C}\right) = \pi - 2\sin^{-1}\left[0.5\frac{d_{sec}}{C}(1-i)\right] \quad (6)$$

$$\beta_{sec} = \pi + 2\sin^{-1}\left(\frac{d_{sec} - d_{pri}}{2C}\right) = \pi + 2\sin^{-1}\left[0.5\frac{d_{sec}}{C}(1-i)\right] \quad (7)$$

STEADY STATE MODEL OF A METAL V-BELT CVT - KINETICS OF PUSH BELT CVT

The CVT system runs at a steady state condition i.e. constant transmission ratio. The driver and driven pulleys run at constant angular velocities and are subjected to loading conditions of torques and axial forces. The belt inertial effects have been neglected, except for the terms arising from the centripetal acceleration of the belt.

Fig. 3 shows the geometry of the band pack around a number of belt segments while traveling around a pulley wrap angle. Tangential slip is modeled on the basis of gap redistribution between the belt elements. For the analysis of pushing V-belt, the following assumptions have been made [11], [12]:

$\sum F = 0$ in X-direction

$$(T + dT) \cos \theta = F_F + T \cos \theta \quad (8)$$

$$T \cos \theta + dT \cos \theta = F_F + T \cos \theta$$

Since θ is very small, $\cos \theta = 1$ and $\sin \theta = \theta$, which may be simplified to?

$$F_F = dT \cos \theta \quad (9)$$

$\sum F = 0$ in Y-direction

$$(T + dT) \sin \theta + T \sin \theta = F_N$$

$$F_N = (2T + dT) \sin \theta \quad (10)$$

$\sum F = 0$ in tangential-direction

$$F_T + F_p \cos \theta = (F_p + dF_p) \cos \theta + F_F$$

which may be simplified to

$$F_T = dF_p \cos \theta + F_F \quad (11)$$

$\sum F = 0$ in radial-direction

$$F_N + 2F_R \cos \alpha = F_C + (2F_p + dF_p) \sin \theta + 2N \sin \alpha \quad (12)$$

where: $F_C = m \frac{v^2}{R}$

BELT FRICTION CHARACTERISTICS

The V-belt type CVT utilizes friction to transmit power from the primary pulley to the secondary pulley. The traction curve is the dimensionless relationship between transmitted torque and the slip. The maximum input torque that can be transmitted by the CVT is dependent on the applied clamping force. The belt slips speed and the belt friction coefficient increase when the transmission torques increase. The traction coefficient is therefore chosen to be a dimensionless value [15]. The traction coefficient of primary and secondary side μ_p , μ_s are defined as:

$$\mu_p = \frac{T_p \cos \alpha}{2 F_p R_p} \quad \text{and} \quad \mu_s = \frac{T_s \cos \alpha}{2 F_s R_s} \quad (13)$$

in which T_p , T_s represent the input and output torque, R_p , R_s represent the primary and secondary running radius of the belt on the pulley, F_p , F_s represent the primary and secondary clamping forces and α is the pulley wedge angle.

The transmission efficiency of the CVT is

$$\eta_T = \frac{P_{out}}{P_{inp}} = \frac{\omega_s T_s}{\omega_p T_p} \quad (14)$$

Power loss of the CVT from this equipment is

$$P_{loss} = P_{inp} - P_{out} = \frac{2\pi (n_p T_p - n_s T_s)}{60000} \quad (15)$$

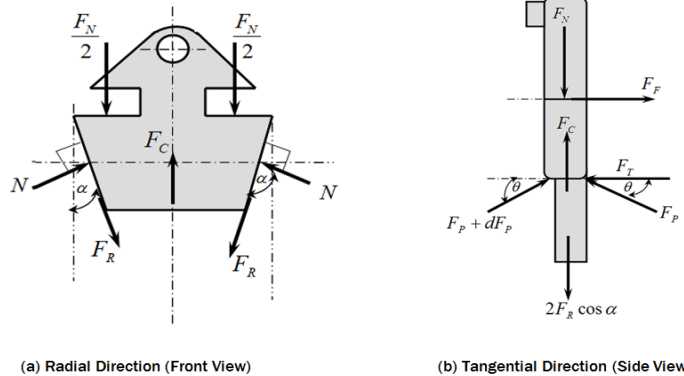


Fig. 3: Free Body Diagram of One Segment

The power loss given by Equ. (15) include slipping losses arising between each contacting component in the CVT, the belt torque loss caused by the resistance to radial resistance and the loss from four bearings supporting the pulley shafts.


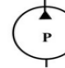
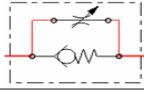
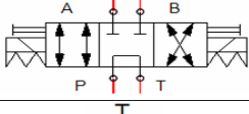

Experimental Work - Test stand setup

Fig. 4 shows the test stand setup for measuring performance of the push belt CVT considered. The experimental work consists of a 25 horsepower (Hp), 3000 rev/min induction motor drawing power and driving a CVT belt system of Mitsubishi lancer GLX vehicle gearbox, a separate hydraulic brake that is couple to the output shaft of the CVT. The schematic diagram of the experimental set up with instrumentation details is shown in Fig. 5. The motor, hydraulic disc brake, CVT gearbox and hydraulic shift system are hard mounted and aligned on a bedplate. The bedplate is mounted using isolation feet to prevent vibration transmission to the floor. The shafts are connected with both flexible and rigid couplings.

HYDRAULIC CIRCUIT AND MEASURING

The measurement methodology used induction (1.5HP, 1450 rev/min) motor drawing power through a electrical source and driving hydraulic pump, the hydraulic shift system characteristics are as follows table 1.

Table 1: Hydraulic system characteristics

No.	Component	Specification	Values	Symbol
1	Drive Motor	Power Voltage Current	1.5 HP 1420 rpm 220/230 V 9.82 Amp	
2	Hydraulic Pump	Flow rate Max. pressure	10Liter/min 10 bar @ 1420 rpm	
3	Choke Valves	Flow rate	15 litre/ min	
4	Directional control valve	Flow rate Operated Position Ports Center	30 liter/min Mechanically Operated 3 position 4 ports Closed Center	
5	Oil Tank	Capacity	Up to 15 liter Capacity	

The hydraulic part of the CVT essentially consists of a gear pump directly connected to the driving electrical motor, the Directional Control Valve (DCV), choke valves and a pressure cylinder of the moveable pulley sheaves. The volume between the pump and the chock valves including the secondary pulley cylinder is referred to as the secondary circuit, the volume directly connected to and plus the primary pulley cylinder is the primary circuit. Excessive flow in the secondary circuit bleeds off towards the accessories, whereas the primary circuit can blow off towards the drain. Pressures are defined relative to the atmospheric drain pressure p_T . The Directional Control Valve (DCV) directs the pressurized fluid to either primary or secondary pulley as set to position A or B. In neutral position the DCV returns the fluid to the tank. The Choke Valves: The Throttle Choke Valve allows the pressure flow normally in the forward direction, and restricts (choke) the flow in the return direction. It is used here to maintain the pressure level in the pulley after shifting the pressure direction to the other pulley, the connection and operation of hydraulic shift system shows in Fig. 6. As the model will only be used to determine the hydraulic system constraints needed for the feed forward control, the following assumptions have been made:

- The compressibility of the oil is neglected
- The oil temperature is constant and all leakage flows are negligible

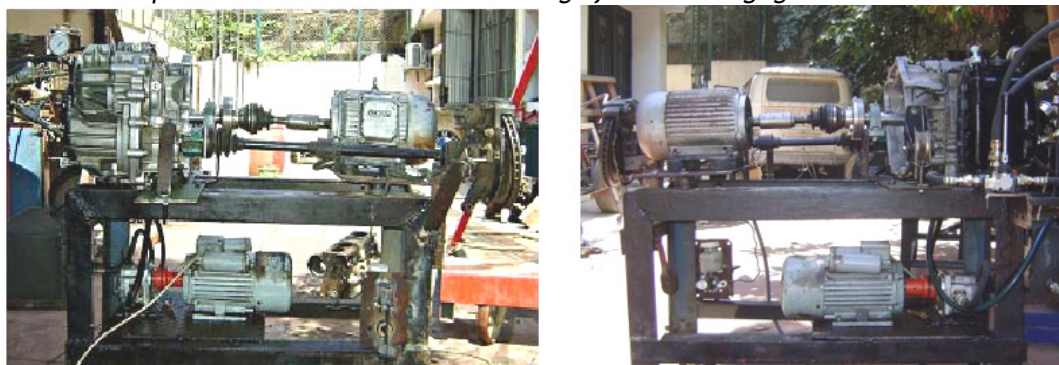


Fig. 4: Photograph of the layout of the test rig

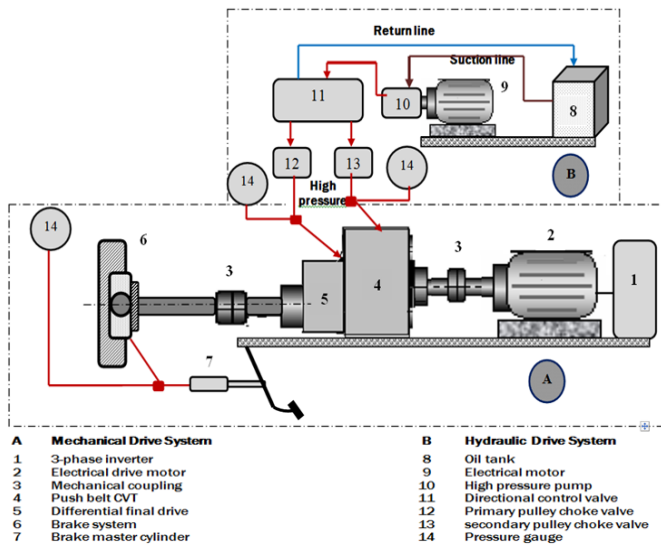


Fig. 5: Test Stand layout

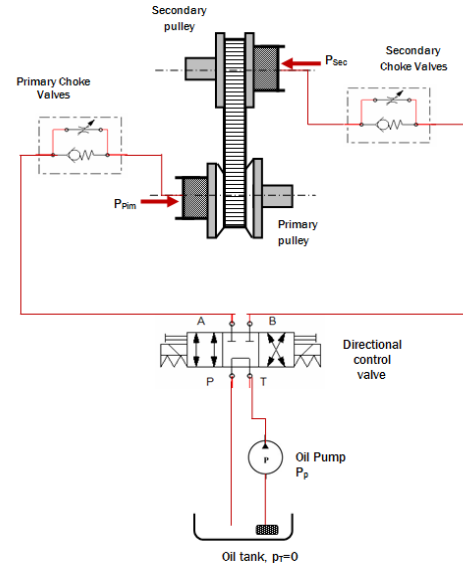


Fig. 6: Schematic Diagram of Hydraulic Control Circuit

The clamping forces F_p and F_s are realized mainly by the hydraulic cylinders on the moveable sheaves. Since the cylinders are an integral part of the pulleys, they rotate with an often very high speed, so centrifugal effects have to be taken into account and the pressure in the cylinders will not be homogeneous. Therefore, the clamping forces will also depend on the pulley speeds ω_{pri} and ω_{sec} . Furthermore, a prestressed linear elastic spring with stiffness K_s is attached to the moveable secondary sheave. This spring has to guarantee a minimal clamping force when the hydraulic system fails. Together this results in the following relations for the clamping forces:

$$F_p = P_p * A_p + C_p * \omega_{pri}^2 \quad (16)$$

Here, A_p is the primary piston area, C_p a centrifugal coefficient and P_p the oil pressure in the primary circuit.

$$F_s = P_s * A_s + C_s * \omega_{sec}^2 + K_s \Delta x + F_i \quad (17)$$

Likewise, the secondary pulley clamping force F_s consists of a direct pressure term $P_s * A_s$ and a centrifugal force. with A_s the secondary piston surface, C_s the centrifugal coefficient and P_s the secondary pressure. Moreover, in F_s there is a contribution of the secondary spring F_{spr} that has to warrant a minimal clamping force under all circumstances. F_i is the force in the spring if the secondary moveable sheave is at position $\Delta x = 0$. The oil flow from the (DCV) to the primary circuit, by use the law of mass conservation, applied to the primary circuit:

$$Q_{DCV \rightarrow p} = C_f * A_p * x_p \sqrt{\frac{2(p_s - p_p)}{\rho}} \text{sign}(p_s - p_p) \quad (18)$$

where C_f is a constant flow coefficient and ρ is the oil density. The equivalent valve opening area A_{sp} depends on the primary valve stem position x_p . The oil flow from the primary circuit to the drain

$$Q_{p \rightarrow d} = C_f * A_{pd} * x_p \sqrt{\frac{2(p_p)}{\rho}} \quad (19)$$

A_{pd} is the equivalent opening area of the primary valve for the flow from primary circuit to the drain.

The oil flow from the (DCV) to the secondary circuit, by use the law of mass conservation, applied to the secondary circuit

$$Q_{DCV \rightarrow s} = C_f * A_s * x_s \sqrt{\frac{2(p_p - p_s)}{\rho}} \text{sign}(p_p - p_s) \quad (20)$$

Application of the law of mass conservation to the hydraulic circuit yields, the flow rate of oil pump is written as:

$$Q_{pump} = Q_{DCV \rightarrow s} + Q_{DCV \rightarrow p} + Q_{p \rightarrow d} \quad (21)$$

RMS is a kind of average of pressure and clamping force signal, for discrete signals, the RMS value is defined as:

$$RMS = \sqrt{\frac{1}{N} \sum_{n=1}^N (x(n) - \bar{x})^2} \quad \text{and} \quad \bar{x} = \frac{1}{N} \sum_{n=1}^N x(n) \quad (22)$$

N is the number of samples taken within the signal and $x(n)$ the time domain signal and \bar{x} is the mean value of all the amplitudes.

MODELLING RESULTS

The simulations were conducted on MATLAB platform. The model required the input of design or configuration parameters. The characteristics of the metal belt CVT that influence its response to the loading conditions numerous simulations were done for different loading conditions in order to understand the dynamics of CVT under steady-state conditions. The impending motion in the model is such that the belt starts to move downwards in the driver pulley sheave and upwards in the driven pulley sheave. The transmission ratio for the model is defined as the ratio of belt pitch radius on driver pulley to belt pitch radius on driven pulley.

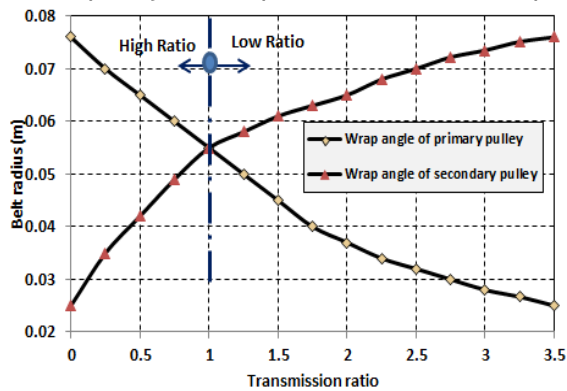


Fig. 7: Belt Radii with transmission ratio

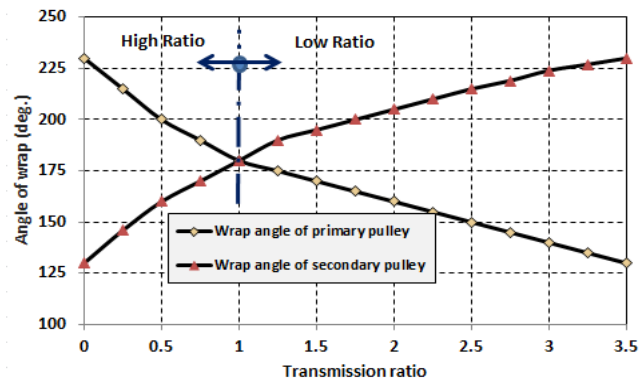


Fig. 8: Variator Wrap Angles with transmission ratio

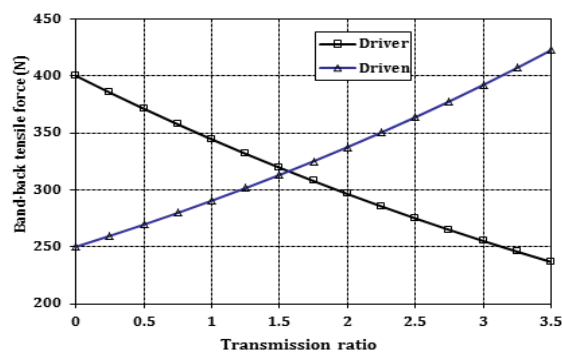


Fig. 9: Band pack tensile force on the driver and driven pulleys

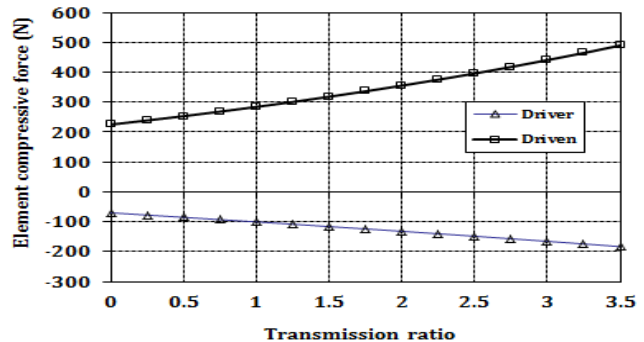


Fig. 10: Belt element compressive force on the driver and driven pulleys

Fig. 7 and Fig. 8 show the calculated pulley radii and angles of wrap about each pulley respectively for the complete range of ratios. Using the ratio definition described above a 'high ratio' or 'overdrive' condition is described by a ratio value (i) of less than one.

The simulation result with constant value of input speed 1600 rpm and torque 120 N.m as illustrate in Figs. 9 and Fig. 10, in Fig. 9 show the tensile force profiles for the band pack on the driver and driven pulleys. The band tensile force decreases from the inlet to the exit of the driver pulley, whereas, it increases from the inlet to the exit of the driven pulley. The elements pack up as the belt moves around the pulleys, and consequently the compressive force in the belt increases. Fig. 10 shows the compressive force profiles on both the driver and the driven sides. It is noted from the figure that there exists a region over the pulley wrap where the compressive force does not build up, this is the inactive arc region.

Practical Results

This section will present the results obtained from the tests carried on the push belt CVT system in the laboratory. The results will be discussed to determining the performance and response of push belt include different oil pressure and transmission ratio. A National Instruments LabVIEW™ program version 7.1 was used to create the desire software program to perform the tests required. The speed variation can be accomplished by varying the frequency to the motor with a AC inverter unit. The motor shaft speed from 800 rpm to 2400 rpm; and the load variation values by hydraulic brake system from zero to 75 N.m.

Fig. 11 and Fig. 12 show the samples from the translation primary and secondary pressure responses in terms of time-domain, with different input speed 800 and 2400 rpm.

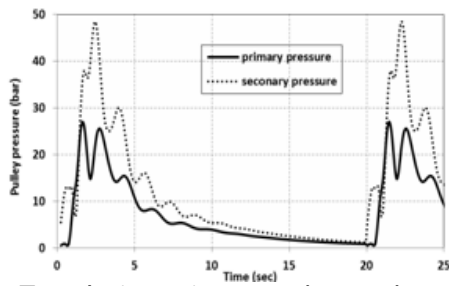


Fig. 11: Translation primary and secondary pressure responses at $\omega_p=800rpm$

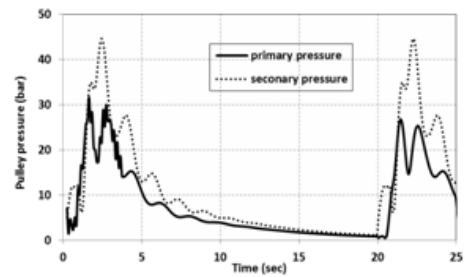


Fig. 12: Translation primary and secondary pressure responses at $\omega_p=2400rpm$

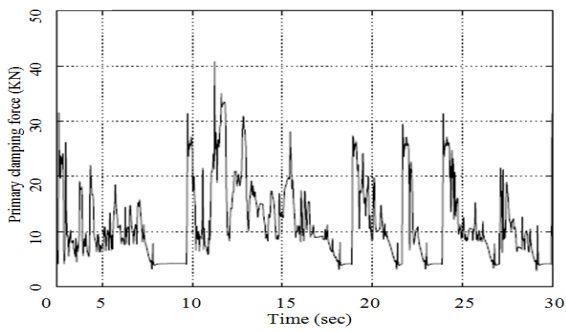


Fig. 13: The primary and secondary clamping force responses at $\omega_p=800rpm$

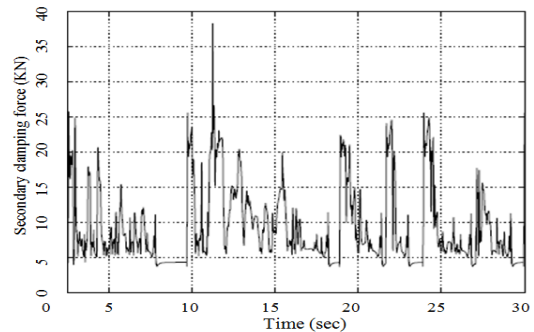
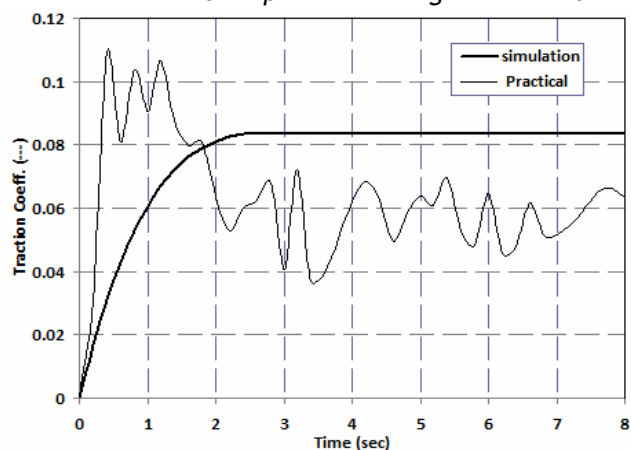
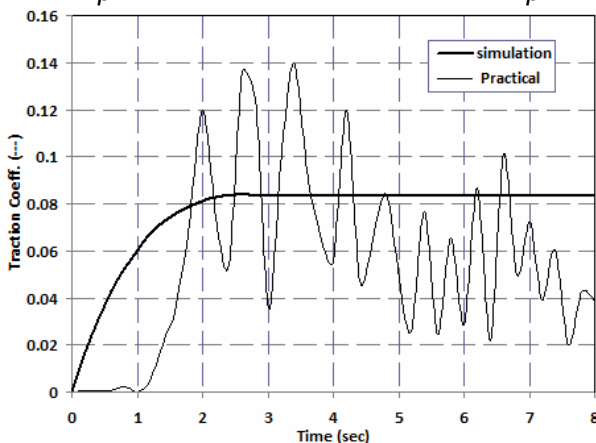


Fig. 14: The primary and secondary clamping force responses at $\omega_p=2400rpm$

Fig. 13 and Fig. 14 show the samples from the translation primary and secondary clamping responses in terms of time-domain. And the other results show in the section comparison of result. The comparison between theoretical and experimental results at 1600 rpm show in Figs. 15 and 16.



High ratio $i=2.6$ overdrive $i= 0.8$

Fig. 15: Comparison between simulation and practical traction coefficient $\omega_p=1600rpm$

Fig. 15 shows the Traction coeff. at different transmission ratios. The efficiency depends on oil pressure, transmission ratio and input speed. Fig. 16 illustrates the transmission efficiency at $i=2.6$. the maximum value of efficiency equal 94% at theoretical and $90 \pm 2\%$ at experimental.

Figs. 17 and 18 illustrate the RMS of clamping force with different output load and different speed and $i=2.6$. Fig. 19 illustrates the maximum value of transmission efficiency with different clamping force.

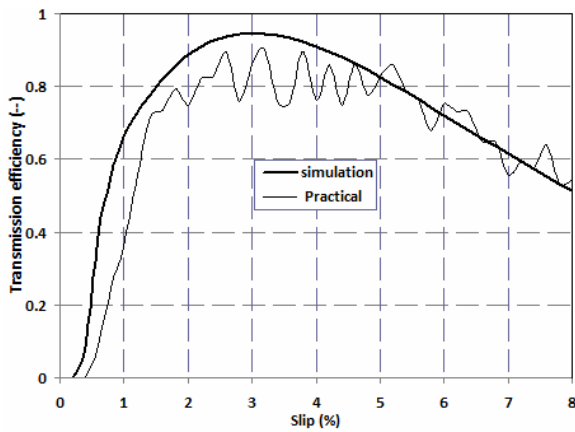


Fig. 16: Comparison between simulation and practical of transmission efficiency

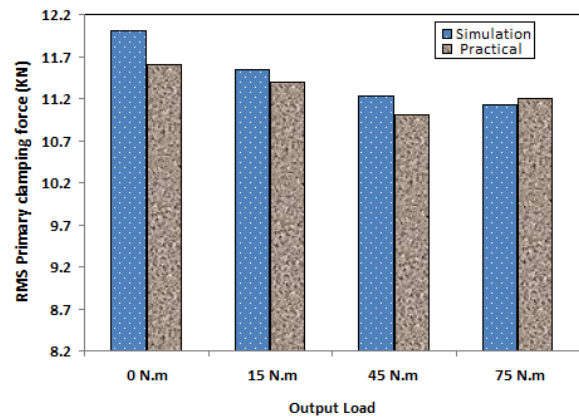


Fig. 17: Comparison between simulation and practical of clamping force RMS

$\omega_p = 1600\text{rpm}$

$\omega_p = 1600\text{rpm}$

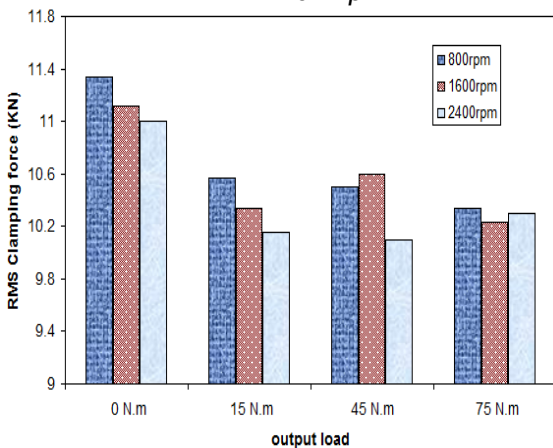


Fig. 18: RMS of practical clamping force with different input speed

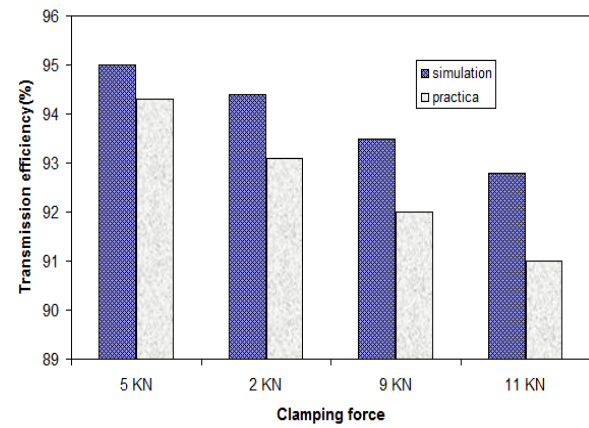


Fig. 19: Comparison between simulation and practical of maximum transmission efficiency with different clamping force

CONCLUSIONS AND RECOMMENDATIONS

In this paper, we present the dynamic analysis and experimental evaluation of a one type of CVT. The main conclusions from the work carried out summarized in the following points:

1. Applying the different input variable parameters to the bush belt full system mathematical model which are the input speed (ω_p), the transmission ratio (i), the half pulley wedge angle (θ), and the slip ratio, that directly affects the system transmission performance.
2. Based on the RMS of applied pressure and clamping force of CVT gearbox, the influence of changing gearbox speed and load on the RMS value is also introduced, which confirm the discussion stated above.
3. The laboratory apparatus and experimental methodology capability established in this work could be utilized for evaluating the dynamic performance of the push belt CVT.
4. The investigated the reliability of the improved model with a theoretical-experimental comparison of a belt drive variator in steady state conditions. Our calculations have shown a good agreement between theory and experiments especially at high clamping forces values, either in predicting the thrust force ratio necessary to establish the desired transmission ratio either in evaluating the variator traction behaviour.

Nomenclature

T	The band tension. (The total tension in both band packs.) (N)
FI	Inertia Force (N)
$T1, T2$	Belt Tensions at ends of the Element (N)
F_c	Centrifugal Force (N)
FF	Friction force acting between band pack and segment or between neighboring bands (N)
FN	Total normal force acting on the segment shoulder (N)
FT	The tangential friction force acting between the pulley surface and the segment side (N)
FR	Radial friction force acting between the pulley surface and the segment sides (N)
F_{axle}	Axial force acting on the segment(N)
m	Mass of one belt segment(Kg)
v	The velocity of the segment (m/s)

R	The rolling radius of the belt segment(m)
R_{sec}	Radius of the secondary bulley (m)
R_{pr}	Radius of the primary bulley (m)
C	Center distance (m)
β_{pri}	Contact angle for primary pulley (deg)
β_{sec}	Contact angle for secondary pulley (deg)
i	Transmission ratio
L	Belt Length (m)
P_p, P_s	Primary and secondary oil pressure (bar)
F_s, F_p	Secondary and primary clamping force(N)
A_p, A_s	Primary and secondary pistons area (m ²)
ω_p, ω_s	Primary and secondary velocities (r/s)

REFERENCES

- [1] Lingyuan Kong, Robert G. Parker “Steady mechanics of layered, multi-band belt drive used in continuously variable transmissions (CVT)” *science direct Mechanism and Machine Theory* 43 (2008) 171-185.
- [2] Shinya k., Toru fujii, shigera K. “Study on a Metal pushing V-belt Type CVT: Band Tension and Load Distribution in Steel rings” *EISEVIER*, March 1999, *JSAE* 20(1999)55-60.
- [3] Shafie, and M. H. Ali “Development of an Efficient CVT using Electromechanically System” *World Academy of Science, Engineering and Technology* 56, 2009.
- [4] Mohan Gangadurl, N. Harikrishnan and b. sreekumar” *Development of an Analytical Design Concept of Mechanical Controlled continuously Variable Transmission* *SAE*, 2005-26-069.
- [5] B.Bonsen, T.W.G.L. Klaassen, K.G.O. van de Meerakker” *Modeling Slip- and Creep-mode Shift Speed Characteristics of a Push-belt Type Continuously Variable Transmission* *04CVT-3*
- [6] Allen, Mark and LeMaster, Robert. “A Hybrid Transmission for SAE Mini Baja Vehicles”. *SAE Publication* 2003-32-0045.
- [7] Micklem J. D., Longmore D. K., Burrows C. R., “Modeling of the Steel Pushing V-belt Continuously Variable Transmission”, *Proceedings Inst. Mech. Engineers Vol. 208 Part C*: pp. 13-27.
- [8] Shimizu H., Kobayashi D., Kawashima J., Kato Y., “Development of 3-D Simulation for Analyzing the Dynamic Behavior of a Metal Pushing V-Belt for CVTs”, *SAE Paper*, 2000-01-0828, *SAE special publication (SP-1522)*, transmission and driveline symposium 2000, pp. 31-36.
- [9] M. Kurosawa, M. Kobayashi and M. Tominaga “Development of a High Torque Capacity Belt Derive CVT with a Torque Converter” *EISEVIER*, July 1998, *JSAE* 20(1999)281-287.
- [10] Bert Pennings, Mark van D., Arjen B., Erik van G. and Marlène L. “Van Doorne CVT Fluid Test: A Test Method on Belt-Pulley Level to Select Fluids for Push Belt CVT. Applications” *2003 SAE International P.N* 2003-01-3253.
- [11] Christopher Ryan Willis “A Kinematic Analysis and Design of a Continuously Variable Transmission” *Master of Science in Mechanical Engineering*, 19 January 2006.
- [12] Zhijian Lu “Acceleration Simulation of a Vehicle with a Continuously Variable Power Split Transmission” *Master of Science in Mechanical Engineering*, July 29, 1998

ANNALS of Faculty Engineering Hunedoara



- International Journal of Engineering

copyright © UNIVERSITY POLITEHNICA TIMISOARA,
FACULTY OF ENGINEERING HUNEDOARA,
5, REVOLUTIEI, 331128, HUNEDOARA, ROMANIA
<http://annals.fih.upt.ro>